Biochimica et Biophysica Acta 1837 (2014) 139–148

Contents lists available at ScienceDirect

Biochimica et Biophysica Acta

journal homepage: www.elsevier.com/locate/bbabio

Modification of the pheophytin redox potential in *Thermosynechococcus elongatus* Photosystem II with PsbA3 as D1

Miwa Sugiura [a,b,*], Chizuko Azami [a], Kazumi Koyama [a], A. William Rutherford [c], Fabrice Rappaport [d], Alain Boussac [e,**]

[a] Proteo-Science Research Center, Ehime University, Bunkyo-cho, Matsuyama, Ehime 790-8577, Japan
[b] PRESTO, Science and Technology Agency (JST), 4-1-8, Honcho, Kawaguchi, Saitama 332-0012, Japan
[c] Department of Life Sciences, Imperial College London, London SW7 2AZ, UK
[d] Institut de Biologie Physico-Chimique, UMR 7141 CNRS and Université Pierre et Marie Curie, 13 rue Pierre et Marie Curie, 75005 Paris, France
[e] iBiTec-S, CNRS UMR 8221, CEA Saclay, 91191 Gif-sur-Yvette, France

ARTICLE INFO

Article history:
Received 8 July 2013
Received in revised form 12 September 2013
Accepted 13 September 2013
Available online 20 September 2013

Keywords:
Photosystem II
PsbA
Thermosynechococcus elongatus
Cyanobacterium
Pheophytin
Singlet oxygen

ABSTRACT

In Photosystem II (PSII) of the cyanobacterium *Thermosynechococcus elongatus*, glutamate 130 in the high-light variant of the D1-subunit (PsbA3) was changed to glutamine in a strain lacking the two other genes for D1, *psbA*$_1$ and *psbA*$_2$. The resulting PSII (PsbA3/Glu130Gln) was compared with those from the "native" high-light (PsbA3-PSII) and low-light (PsbA1-PSII) variants, which differ by 21 amino acid including Glu130Gln. H-bonding from D1-Glu130Gln to the primary electron acceptor, Pheophytin$_{D1}$ (Pheo$_{D1}$), is known to affect the E_m of the Pheo$_{D1}$/Pheo$_{D1}^{-\bullet}$ couple. The Gln130 mutation here had little effect on water splitting, charge accumulation and photosensitivity but did slow down $S_2Q_A^{-\bullet}$ charge recombination and up-shift the thermoluminescence while increasing its yield. These changes were consistent with a ≈ -30 mV shift of the Pheo$_{D1}$/Pheo$_{D1}^{-\bullet}$ E_m, similar to earlier single site-mutation results from other species and double the ≈ -17 mV shift seen for PsbA1-PSII versus PsbA3-PSII. This is attributed to the influence of the other 20 amino-acids that differ in PsbA3. A computational model for simulating $S_2Q_A^{-\bullet}$ recombination matched the experimental trend: the $S_2Q_A^{-\bullet}$ recombination rate in PsbA1-PSII differed only slightly from that in PsbA3-PSII, while in Glu130-PsbA3-PSII there was a more pronounced slowdown of the radical pair decay. The simulation predicted a major effect of the Pheo$_{D1}$/Pheo$_{D1}^{-\bullet}$ potential on $^1O_2$ yield (~60% in PsbA1-PSII, ~20% in PsbA3-PSII and ~7% in Gln130-PsbA3-PSII), reflecting differential sensitivities to high light.

1. Introduction

The light-driven oxidation of water in PSII is the first step in the photosynthetic production of biomass, fossil fuels and O_2 on Earth. PSII is made up of 17 membrane protein subunits and 3 extrinsic proteins. Altogether these bear 35 chlorophylls, 2 pheophytins (Phe), 2 hemes, 1 non-heme iron, 2 plastoquinones (Q_A and Q_B), 1 Mn_4CaO_5 cluster, 2 Cl^-, 12 carotenoids and 25 lipids [1]. The excitation resulting from the absorption of a photon is transferred to the photochemical trap that undergoes charge separation. The positive charge is then stabilized on P_{680} which is composed of four chlorophyll *a* molecules, P_{D1}/P_{D2} and Chl_{D1}/Chl_{D2}, and two pheophytin *a* molecules, $Pheo_{D1}/Pheo_{D2}$. Then, $P_{680}^{+\bullet}$ oxidizes Tyr_Z, the Tyr161 of the D1 polypeptide, which in turn oxidizes the Mn_4CaO_5 cluster. On the electron acceptor side the electron is transferred to the primary quinone electron acceptor, Q_A, and then to Q_B, a two-electron and two-proton acceptor, e.g. [2–5]. The Mn_4CaO_5 cluster both accumulates oxidizing equivalents and acts as the catalytic site for water oxidation. The enzyme cycles sequentially through five redox states, denoted S_n where n stands for the number of stored oxidizing equivalents. Upon formation of the S_4 state two molecules of water are rapidly oxidized, the S_0 state is regenerated and O_2 released, e.g. [6–11]. See also [12–14] for energetic considerations.

Cyanobacterial species have multiple *psbA* variants coding for the D1 protein, e.g. [15–25]. These different genes are known to be differentially expressed depending on the environmental conditions, e.g. [15–23]. In particular, specific up/down-regulations of one of these genes under high light conditions is indicative of a photo-protection mechanism. For example, the mesophilic cyanobacterium, *Synechocystis* PCC 6803, has three *psbA* genes. Although *psbAII* and *psbAIII* produce an identical D1, *psbAII* is expressed under the standard cultivation

Abbreviations: PSII, Photosystem II; Chl, chlorophyll; MES, 2-(N-morpholino) ethanesulfonic acid; P_{680}, chlorophyll dimer acting as the second electron donor; Q_A, primary quinone acceptor; Q_B, secondary quinone acceptor; 43H, *T. elongatus* strain with a His-tag on the C terminus of CP43; PQ, plastoquinone 9; WT*1, WT*2, WT*3, cells containing only the *psbA*$_1$, *psbA*$_2$, *psbA*$_3$ gene, respectively; $Pheo_{D1}$, pheophytin; P_{D1} and P_{D2}, Chl monomer of P_{680} on the D1 or D2 side, respectively; E_m, redox potential versus SHE; TL, Thermoluminescence; DCMU, 3-(3,4-dichlorophenyl)-1,1-dimethylurea; PPBQ, phenyl p-benzoquinone; β-DM, n-dodecyl-β-maltoside

* Correspondence to: M. Sugiura, Proteo-Science Research Center, Ehime University, Bunkyo-cho, Matsuyama, Ehime 790-8577, Japan. Tel./fax: +81 89 927 9616.
** Corresponding author. Tel.: +33 1 69 08 72 06; fax: +33 1 69 08 87 17.
E-mail addresses: miwa.sugiura@ehime-u.ac.jp (M. Sugiura), alain.boussac@cea.fr (A. Boussac).

0005-2728/$ – see front matter © 2013 Elsevier B.V. All rights reserved.
http://dx.doi.org/10.1016/j.bbabio.2013.09.009

conditions, transcription of *psbAIII* is induced by high light or UV light [18] and that of *psbAI* seems triggered by micro-aerobic conditions [21]. *Thermosynechococcus elongatus* has also three different *psbA* genes in its genome [25]. Among the 344 residues of the PsbA proteins, 21 differ between PsbA1 and PsbA3, 31 between PsbA1 and PsbA2 and 27 between PsbA2 and PsbA3 [25]. It has also been reported that in *T. elongatus psbA*$_1$ is constitutively expressed under standard laboratory conditions, while the transcription of *psbA*$_3$ occurred under high-light or UV light conditions [19,26,27]. Other cryptic *psbA* genes were found to be induced in micro-aerobic conditions [28,29]. A class of "rogue" D1 protein has also been recently described [30]. Recent reviews on the cyanobacterial *psbA* gene family [20] and strategies for the *psbA* gene expression are available in the literature [31].

Fig. 1 shows a scheme depicting the energetics and recombination pathways in PSII. In *T. elongatus*, the change of PsbA1 for PsbA3 has been shown to increase the midpoint potential of the $Pheo_{D1}/Pheo_{D1}^{-\bullet}$ couple by 17 mV from −522 mV in PsbA1-PSII [32] to −505 mV in PsbA3-PSII [33] and the midpoint potential of $Q_A/Q_A^{-\bullet}$ by ≈41 mV from −124 mV in PsbA1-PSII to −83 mV in PsbA3-PSII [34]. These changes in the E_m of $Pheo_{D1}/Pheo_{D1}^{-\bullet}$ and $Q_A/Q_A^{-\bullet}$ result in a larger energy gap by 24 meV between the two states $Pheo_{D1}^{-\bullet}Q_A$ and $Pheo_{D1}Q_A^{-\bullet}$ in PsbA3-PSII than in PsbA1-PSII. All these E_m changes are expected to have several consequences: *i*) an increase in the energy gap between $Pheo_{D1}^{-\bullet}Q_A$ and $Pheo_{D1}Q_A^{-\bullet}$ would lead to a less efficient repopulation of $Pheo_{D1}^{-\bullet}Q_A$ [35]; *ii*) the direct route $P_{680}^{+\bullet}Q_A^{-\bullet}$ to $P_{680}Q_A$, which very likely occurs in the Marcus inverted region, would be faster when the E_m of the $Q_A/Q_A^{-\bullet}$ couple increases (this seems likely since there is an experimental evidence indicating that $Tyr_Z^{\bullet}(H^+)Q_A^{-\bullet}$ to Tyr_ZQ_A charge recombination, which has a smaller driving force, occurs in the Marcus inverted region [36]), and *iii*) the indirect route in the $P_{680}^{+\bullet}Pheo_{D1}^{-\bullet}$ to $P_{680}Pheo_{D1}$ charge recombination, which also very likely occurs in the Marcus inverted region [37], would be faster when the E_m of the $Pheo_{D1}/Pheo_{D1}^{-\bullet}$ couple increases. Consequently, *i*) the repopulation of the $Pheo_{D1}^{-\bullet}Q_A$ state from the $Pheo_{D1}Q_A^{-\bullet}$ is expected to be less efficient in PsbA3-PSII than in PsbA1-PSII state and *ii*) the direct route in the $P_{680}^{+\bullet}Q_A^{-\bullet}$ to $P_{680}Q_A$ is expected to be faster in PsbA3-PSII than in PsbA1-PSII (note that at room temperature the $S_{n+1}Q_A^{-\bullet}$ to S_nQ_A charge recombination is thought to occur by repopulating the higher energy radical pairs e.g. $P_{680}^{+\bullet}Q_A^{-\bullet}$ and $P_{680}^{+\bullet}Pheo_{D1}^{-\bullet}$). These two effects would combine in decreasing the production of harmful $^1O_2$ from $^3P_{680}$ formed by charge recombination in the thermally repopulated $^3[P_{680}^{+\bullet}Pheo_{D1}^{-\bullet}]$ state in PsbA3-PSII under light conditions when the accumulation of $Q_A^{-\bullet}$ occurs (see [38] for a discussion).

The finding that *i*) the increase of the E_m of the $Pheo_{D1}/Pheo_{D1}^{-\bullet}$ couple in PsbA3-PSII was half that observed upon single site-directed mutagenesis in *Synechocystis* PCC 6803 [39,40] and *ii*) the $S_2Q_A^{-\bullet}$ charge recombination kinetics were similar in PsbA3-PSII and PsbA1-PSII led us to propose that the effects of the D1-Q130 to E130 substitution on the E_m of $Pheo_{D1}/Pheo_{D1}^{-\bullet}$ could be, at least in part, compensated for by some of the additional amino-acid changes associated with the PsbA3 for PsbA1 substitution [22]. To test this hypothesis and to study the specific effects due to a change of the E_m of the $Pheo_{D1}/Pheo_{D1}^{-\bullet}$ couple we have studied the effect of the E130Q single site-directed mutagenesis in PsbA3-PSII. For earlier studies of related mutation in other organisms see e.g. [41,42].

2. Materials and methods

The construction of the *ΔpsbA*$_1$*ΔpsbA*$_2$ and *ΔpsbA*$_2$*ΔpsbA*$_3$ *T. elongatus* deletion mutants, WT*3 and WT*1 respectively, has been previously described [43,44]. For making the WT*3/E130Q site-directed mutant, the position around +382 of *psbA*$_3$ was modified on the plasmid for PsbA3 mutation [43] by a Quick-Change XL Site-Directed Mutagenesis Kit (Stratagene) as shown in Fig. 2A. Segregation of all the *psbA*$_3$ copies in genome of the deletion mutant was confirmed by the digestion of *psbA*$_3$ with *Sal* I after PCR amplification of the mutated region including the promoter region by using the *P3* (5′-GGCTGGTT CGGCGTGTTGATGATCCCCACT-3′) and *P4* primers (5′-AACCGTAGTTG GCAGATTCGGTTTCGGTGG-3′) (Fig. 2B and C). Finally, the genomic DNA sequences including the mutated regions were confirmed by sequencing by using a GenomeLab GeXP DNA sequencer (Beckman Coulter). The transformation of *T. elongatus* cells was done by electroporation (BioRad gene pulser). The segregated cells were selected as single colonies on DTN agar plates containing 25 μg mL^{-1} of spectinomycin, 10 μg mL^{-1} of streptomycin, 40 μg mL^{-1} of kanamycin and 5 μg mL^{-1} of chloramphenicol as described in [43].

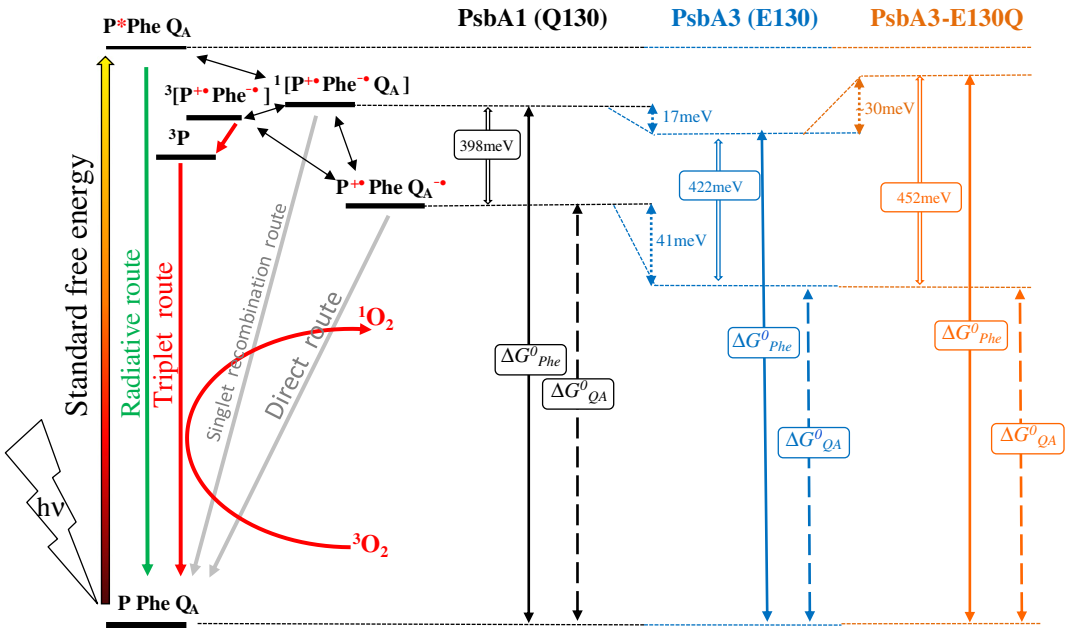

Fig. 1. Scheme depicting the energetics and recombination pathways in PSII. The energy gaps are not to scale but actual values are shown for the most relevant cases for each of the three cases studied and these are color coded black for PsbA1-PSII, blue PsbA3-PSII and orange for PsbA3/E130Q-PSII mutant. For simplicity only the charge recombination from $P_{680}^{+\bullet}Q_A^{-\bullet}$ is shown but this is formed from recombination of more stable charge pairs involving Tyr_Z, the S-states of the water splitting cycle and when is absent Q_B. See the text for more details.

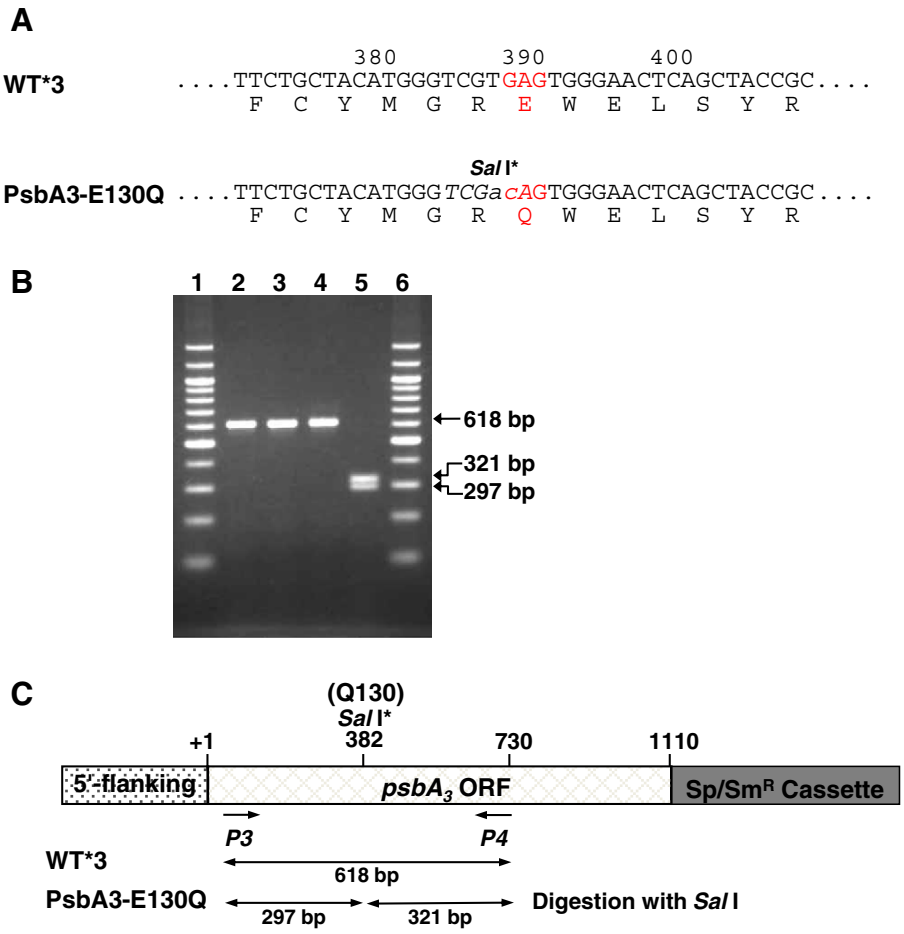

Fig. 2. Construction and confirmation of site-directed mutant strains WT*3-E130Q in the *psbA*$_3$ gene. (A) Nucleotide sequence of *psbA*$_3$ and the deduced amino acid sequences around E130 of WT* and PsbA3 (WT*3)-E130Q. Positions E130 and Q130 are indicated with red letters. Numbers correspond to the position from the initial codon. Substituted nucleotides in the mutant are indicated in small letters. For the selection of mutants, the *Sal* I recognition site (letters in italic) was created in PsbA3-E130. (B) Agarose gel (2%) electrophoresis of PCR products using the *P3* and *P4* primers (lanes 2 and 4) and the products after digestion with *Sal* I (lanes 3 and 5). Lanes 1 and 6, 100 bp DNA ladder markers (Toyobo, Japan); lanes 2 and 3, WT*3 strain; lanes 4 and 5, WT*3-E130Q strain. (C) Physical map around *psbA*$_3$ and theoretical DNA length after treating with *Sac* I the PCR products by using primers *P3* and *P4*. The created *Sal* I (shown as *Sac* I*) site for E130Q mutant is at position +382. Digestion of products from E130Q mutant with *Sal* I generated fragments at 321-bp and 297-bp as shown in Fig. 2B.

Cells were grown in 1 L of DTN in 3-L Erlenmeyer flasks in a rotary shaker with a CO_2-enriched atmosphere at 45 °C under continuous light (≈80 μmol of photons m^{-2} s^{-1}) until they reached an optical density (O.D.) close to 1.0 at 800 nm. After harvesting by centrifugation, the cells were washed once with buffer 1 (1 M betaine, 10% glycerol, 40 mM MES, 15 mM $MgCl_2$, 15 mM $CaCl_2$, pH 6.5 (adjusted with NaOH)) and resuspended in the same buffer, with 0.2% (w/v) bovine serum albumin, 1 mM benzamidine, 1 mM ε-aminocaproic acid, and ≈50 μg mL^{-1} DNase I added, to a chlorophyll concentration of ≈1.5 mg Chl mL^{-1}. The cells were ruptured with a French press. Unbroken cells were removed by centrifugation (3000 *g*, 5 min). Membranes were pelleted by centrifugation at 180,000 *g* for 30 min at 4 °C and washed twice with buffer 1. Thylakoids (1 mg Chl mL^{-1}, final concentration after the addition of the detergent) were treated with 0.8% (w/v) n-dodecyl-β-maltoside (β-DM, Biomol, Germany) in buffer 1 supplemented with 100 mM NaCl. After ≈1 min of stirring in the dark at 4 °C the suspension was centrifuged (20 min, 170,000 *g*) to remove the non-solubilized material. Then, the supernatant was mixed with an equal volume of ProBond resin (Invitrogen, Groningen, The Netherlands) that had been pre-equilibrated with buffer 1. The resulting slurry was transferred to an empty column. After sedimentation of the resin inside the column, the supernatant was removed. The resin was washed with buffer 2 (1 M betaine, 10% glycerol, 40 mM MES, 15 mM $MgCl_2$, 15 mM $CaCl_2$, 100 mM NaCl, 1 mM L-histidine, 0.03% (w/v) β-DM, pH 6.5) until the O.D. value of the eluate at ≈665 nm decreased below 0.05 (approximately 15 h). Then, PSII core complexes were eluted with buffer 3 (1 M betaine, 40 mM MES, 15 mM $MgCl_2$, 15 mM $CaCl_2$, 200 mM NaCl, 180 mM L-histidine, 0.06% (w/v) β-DM, pH 6.5). The eluate was then concentrated and washed in buffer 4 with 1 M betaine, 40 mM MES, 15 mM $MgCl_2$, 15 mM $CaCl_2$, pH 6.5, using centrifugal filter devices (Ultrafree-15, Millipore). PSII core complexes were finally resuspended in the same buffer at a Chl concentration of ≈1.5–2.0 mg Chl mL^{-1} and stored in liquid N_2 before to be used.

Thermoluminescence (TL) glow curves were measured with a lab-built apparatus [45,46]. PSII core complexes were diluted to 10 μg Chl mL^{-1} in 1 M betaine, 40 mM MES, 15 mM $MgCl_2$, 15 mM $CaCl_2$, pH 6.5 and then dark-adapted for 1 h at room temperature. Just before loading the sample, 10 μM DCMU was added to the dark-adapted samples. The samples were illuminated at 1 °C by using a saturating xenon flash. Immediately after the flash, the samples were heated at the constant rate indicated in the legend of the figures and TL emission was detected.

Absorption changes were measured with a lab-built spectrophotometer [47] where the absorption changes are sampled at discrete times by short flashes. These flashes were provided by a neodymium:yttrium–aluminum garnet (Nd:YAG, 355 nm) pumped optical parametric oscillator, which produces monochromatic flashes (1 nm full-width at half-maximum) with a duration of 5 ns. Excitation was provided by a second neodymium:yttrium–aluminum garnet (Nd:YAG, 532 nm) pumped optical parametric oscillator, which produces monochromatic saturating flashes at 695 nm (1 nm full-width at half-maximum) with a duration of 5 ns. The path length of the cuvette was 2.5 mm. PSII

was used at 25 μg of Chl mL^{-1} in 1 M betaine, 15 mM $CaCl_2$, 15 mM $MgCl_2$, and 40 mM MES (pH 6.5). PSII were dark-adapted for ≈1 h at room temperature (20–22 °C) before the additions of either 0.1 mM phenyl p-benzoquinone (PPBQ) or 50 μM 3-(3,4-dichlorophenyl)-1,1-dimethylurea (DCMU), both dissolved in dimethyl sulfoxide.

Fluorescence changes were measured with the same spectrophotometer using 480 nm as a probe wavelength to excite fluorescence. The probe pulse was filtered out using a combination of KV550 and RG690 and RG695 (Schott) filters. For kinetic measurements, the time delay between the actinic flash and the detector flash was varied.

To probe the light sensitivity of the WT*3 and WT*3/E130Q cells they were first pre-cultivated until $O.D._{730} \approx 0.7$, i.e. in the exponential phase, at 45 °C under continuous white light (≈60 μmol of photons m^{-2} s^{-1} fluorescent tubes (Grolux, Sylvania)) and fixed on a rotary shaker (120 rpm). Just before the measurements, the cells were diluted to $O.D._{730} = 0.3$ (250 mL final volume) into 500-mL Erlenmeyer flasks. High light illumination was done with fluorescent light tubes (Toshiba Plantlux, Japan, with an emission spectrum more intense between 600 and 700 nm and between 400 nm and 500 nm) with a light intensity equal to ≈800 μmol of photons m^{-2} s^{-1} for the periods indicated in the figures. Then, when indicated, the light intensity was decreased to ≈60 μmol of photons m^{-2} s^{-1}. When added, the concentration of lincomycin was adjusted to 200 μg per mL of culture. It has been checked that a two times larger concentration of lincomycin resulted in similar results showing that the concentration used here was saturating [44].

For the oxygen evolution measurements with whole cells about 30 mL of cells was quickly taken from the 250-mL cultures and then pelleted by centrifugation. After the washing of the cells in 40 mM MES buffer (pH 6.5) containing 15 mM $CaCl_2$ and 15 mM $MgCl_2$, they were suspended in the same buffer at a concentration of 3 μg of Chl mL^{-1}. The O_2 activity was measured at 25 °C by using a Clark type oxygen electrode (Hansatech) with continuous saturating white light through infrared and water filters. The activity was measured over a period of 1.5 min in the presence of 0.5 mM 2,6-dichloro-*p*-benzoquinone (dissolved in dimethyl sulfoxide) as an electron acceptor.

3. Results

Fig. 3 shows in the Q_x absorption region the electrochromic blue shift undergone by $Pheo_{D1}$ upon reduction of Q_A and known as the C-550 bandshift in PsbA1-PSII (blue trace), in PsbA3-PSII (black trace) and in PsbA3/E130Q-PSII (red trace). For these measurements, the samples were first dark-adapted for 1 h at room temperature then, the absorption changes were measured 15 μs after each actinic flash in a series. The data shown in Fig. 3 are the average of the individual absorption changes induced by the 2nd to 7th flashes. The red shift by ≈3.0 nm of the C550 band-shift for the PsbA3-PSII sample, relative to the PsbA1-PSII sample, reflects the stronger hydrogen bond to the ^{1}13-keto of the $Pheo_{D1}$ from the carboxylate group of E130 in PsbA3-PSII than from Q130 in PsbA1-PSII, as previously shown [48,49]. In the PsbA3/E130Q-PSII sample the electrochromic bandshift was similar to that in the PsbA1-PSII sample, showing that the 20 other amino acid substitutions between PsbA1 and PsbA3 have negligible influence on the electrostatic interaction responsible for the C550 electrochromic bandshift.

Fig. 4 shows the amplitude of the absorption changes associated with the stepwise oxidation of the water oxidizing complex in PsbA3-PSII (black squares) and in PsbA3/E130Q-PSII (red circles). The absorption changes were measured at 292 nm [50–52] 200 ms after each flash in a series, i.e. after completion of the reduction of $Tyr_Z^{\bullet}$ by the water oxidizing complex. At this wavelength the reduction of PPBQ does not lead to any absorption changes and the successive oxidation steps of the water oxidizing complex have significant extinction coefficient [50–52]. The pattern, oscillating with a period of four, is clearly observed for both types of PSII preparations with a very similar damping, assuming the same miss parameter (here, ≈10%) on all S-state transitions (not shown).

Thermoluminescence is well suited to probe the E_m of the $Pheo_{D1}/Pheo_{D1}^{-\bullet}$ couple [42,53,54]. In conditions where only the E_m of the $Pheo_{D1}/Pheo_{D1}^{-\bullet}$ couple varies, a more negative value is expected to translate into a higher peak temperature, owing to a larger energy gap between the $Pheo_{D1}^{-\bullet}Q_A$ and the $Pheo_{D1}Q_A^{-\bullet}$ pairs and a larger intensity of the TL glow curve owing to a smaller energy gap between $P_{680}{}^*Pheo_{D1}$ and $P_{680}^{+\bullet}Pheo_{D1}^{-\bullet}$, see [42,53,54] for a detailed explanation of the TL glow curve dependence upon changes of the various energy levels of the radical pairs involved in luminescence.

Fig. 5 shows the TL glow curves arising from the $S_2Q_A^{-\bullet}$ charge recombination in PsbA3-PSII (black trace) and in PsbA3/E130Q-PSII (red trace) in the presence of DCMU as an inhibitor of the reoxidation of $Q_A^{-\bullet}$ by Q_B. The peak temperature T_m was upshifted by ≈14 °C from ≈18 °C in PsbA3-PSII to ≈32 °C in PsbA3/E130Q-PSII and the intensity of the glow curve in PsbA3/E130Q-PSII was approximately twice that in PsbA3-PSII. These effects are very similar to those observed in *Synechocystis* 6803 in which the Q130 to E130 mutation induced a downshift by ≈15 °C of the peak temperature of the glow curve with intensity approximately 4 fold smaller [53].

As discussed in [53,54] when repopulation of the potentially luminescing excited state is the only possible pathway for charge

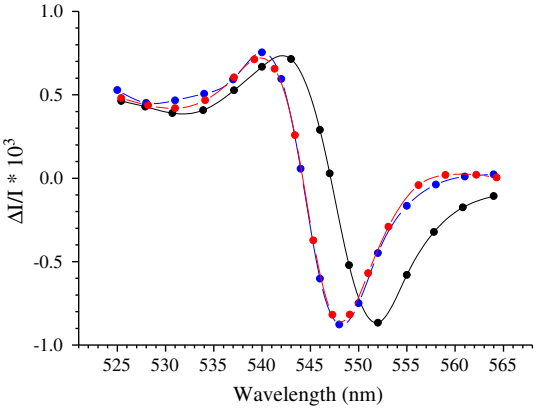

Fig. 3. Light-induced difference spectra around 545 nm. The flash-induced absorption changes were measured in PsbA1-PSII (blue trace) and PsbA3-PSII (black trace) and in PsbA3/E130Q-PSII (red trace). Measurements were performed 15 μs after the flash and were averaged from the 2nd to 7th flash given to dark-adapted PSII. Upon dark-adaptation for 1 h at room temperature, 100 μM PPBQ (dissolved in dimethyl sulfoxide) was added to the samples (Chl concentration was 25 μg mL^{-1}). The difference spectra were normalized to the same amplitude.

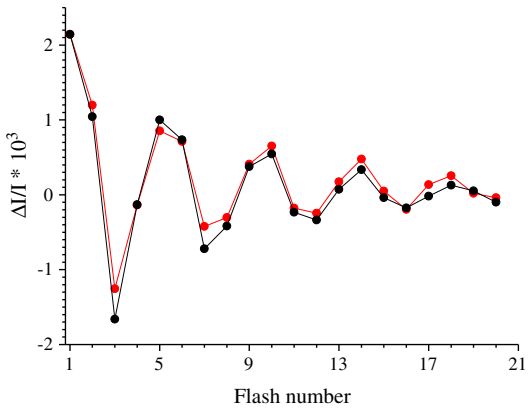

Fig. 4. Sequence of the amplitude of the absorption changes at 292 nm. The measurements were done during a series of saturating flashes (spaced 200 ms apart) given to dark-adapted PsbA3-PSII (black trace) or PsbA3/E130Q-PSII (red trace). The samples ([Chl] = 25 μg mL^{-1}) were dark-adapted for 1 h at room temperature before the addition of 100 μM PPBQ. The measurements were done 200 ms after each flash. The buffer was 1 M betaine, 15 mM $CaCl_2$, 15 mM $MgCl_2$, 40 mM MES, and pH 6.5.

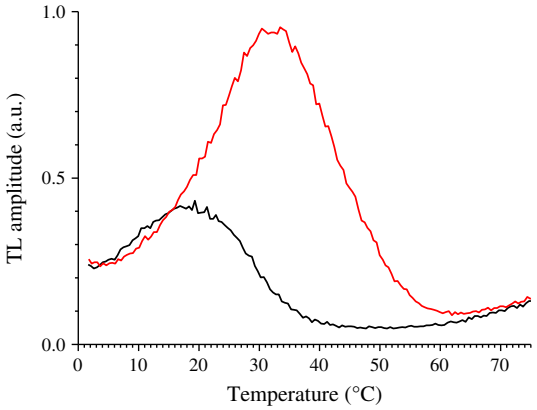

Fig. 5. Thermoluminescence glow curves from $S_2Q_A^{-\bullet}$ charge recombination in the presence of DCMU in PsbA3-PSII (black trace) and in PsbA3/E130Q-PSII (red trace). See Materials and methods section for more details.

recombination, the intensity of the TL curve is proportional to the heating rate. Numerous studies have shown that charge recombination may occur via several competing pathways, e.g. [35,37,38,40,42,53,54] and, as a result, TL intensity in PSII is non-linearly related to the heating rate and the deviation to linearity is all the more pronounced as the relative weight of the non-radiative pathways is important. In PsbA3/E130Q-PSII due to the more negative value of E_m of the $Pheo_{D1}/Pheo_{D1}^{-\bullet}$ couple, the proportion of centers in which the charge recombination occurs by non-radiative pathways is expected to increase as demonstrated earlier [42,53,54]. Indeed, in PsbA3/E130Q-PSII, the curve deviates more pronouncedly from linearity as expected from a larger weight of the non-radiative routes (see Supplementary material).

The comparison of the recombination kinetics in PsbA3-PSII and PsbA3/E130Q-PSII provides another tool to study the different contributions of the thermally activated repopulation of the $P_{680}^{+\bullet}Pheo_{D1}^{-\bullet}$ state to this process in the two samples. Fig. 6 shows the decay of the fluorescence yield after a single saturating flash in the presence of DCMU, in PsbA3-PSII (black symbols) and PsbA3/E130Q-PSII (red symbols). Owing to the non-linear dependence of fluorescence upon the fraction of PSII being in the $Q_A^{-\bullet}$ state, the decay of $Q_A^{-\bullet}$ associated with charge recombination can only be obtained with negligible distortion when using non-saturating flashes [41]. The data shown in Fig. 6 were obtained using an actinic flash hitting about 10–15% PSII's. In line with

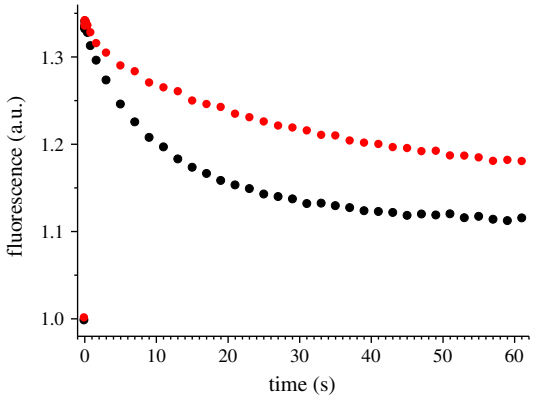

Fig. 6. Fluorescence decay. The dark-adapted samples were illuminated by a non-saturating flash, then the decay was followed by a train of detecting flashes at the indicated times. The measurements were done at room temperature in PsbA3-PSII (black symbols) and in PsbA3/E130Q-PSII (red symbols) in the presence of DCMU. The traces were normalized to the amplitude of the first point measured at 100 ms after the actinic flash. The samples ([Chl] = 25 μg mL^{-1}) were dark-adapted for 1 h at room temperature before the addition of the herbicide (dissolved in dimethyl sulfoxide) at 100 μM.

the previous observations, the $S_2Q_A^{-\bullet}$ decay was about two-fold slower in the mutant than in the control case.

All the results described above are consistent with the E130 to Q130 single site directed mutant having the expected effect on the E_m ($Pheo_{D1}/Pheo_{D1}^{-\bullet}$) value. It is well documented that changes in the E_m of the $Pheo_{D1}/Pheo_{D1}^{-\bullet}$ couple modify the rate of the photodamage of PSII due to the production of $^1O_2$ [37,53], see also [38]. To examine the effect of the E130 to Q130 mutation in PsbA3-PSII, the O_2 evolution activity was measured in WT*3 cells (which express only PsbA3 as D1) and WT*3/E130Q cells (which express the PsbA3/E130Q as D1) after periods from 0 to 4 h under a light intensity close to 800 μmol of photons m^{-2} s^{-1} either in the presence (Fig. 7A) or in the absence (Fig. 7B) of lincomycin, a protein synthesis inhibitor. After incubation for 4 h, the light intensity was decreased to 60 μmol of photons m^{-2} s^{-1}, a growth light intensity routinely used for cell cultivation. These experiments allow us to separately monitor the photo-damage and the repair processes.

In the absence of lincomycin, in WT*3 cells the O_2 evolution decreased during the first hour to a value close to 70% of the starting value and then remained constant during the next 3 h of high light illumination. When the light intensity was decreased after cultivation for 4 h under high light intensity, the activity recovered its original value in ≈1 h. These results are in agreement with those already observed in the same WT*3 cells [44]. In WT*3/E130Q cells, both the O_2 evolution inhibition and recovery occurred with a similar time-course as that obtained with WT*3 cells. In the presence of lincomycin, the O_2 evolution activity decreased to less than 5% of the starting value in both WT*3 cells and WT*3/E130Q cells with very similar kinetics.

In the absence of lincomycin, the same kinetics for the recovery is not unexpected because the same promoter is involved for PsbA3 and PsbA3/E130Q. In contrast, based on the literature, e.g. [55], it would be predicted that WT*3/E130Q cells would be more susceptible to photodamage under high light conditions than WT*3 cells. Experimentally, this turns out not to be the case. Furthermore, after 1 h under high light conditions in the presence of lincomycin, the WT*3/E130Q cells appeared to be very slightly less affected than WT*3 cells (see also the supplementary material). Although this effect is very small it corresponds to an average of 7 experiments which gives it some credibility. To further test this property of WT*3/E130Q cells we have compared their growth rates under various light intensities to those of WT*3 cells (Fig. 8). Whatever the light intensity from 10 to 80 μmol of photons m^{-2} s^{-1}, the growth rate of WT*3-E130Q cells was faster than that of WT*3 cells.

4. Discussion

A change of the midpoint potential of the $Pheo_{D1}/Pheo_{D1}^{-\bullet}$ couple can be achieved by modifying the strength of the hydrogen bond between $Pheo_{D1}$ and the amino acid residue at position 130 in the D1 protein. The consequences of a modification of the value of the E_m of the $Pheo_{D1}/Pheo_{D1}^{-\bullet}$ couple on the electron transfer have been already extensively studied both theoretically and experimentally in the literature, see e.g. [17–19,37–42,53–55] for detailed analysis. The aim of this paper was therefore not to reinvestigate this issue but rather to understand why in *T. elongatus*, the amino acid differences between PsbA1 and PsbA3, which include the Q130 to E130 substitution in addition to 20 other amino acid changes, hardly affect the $S_2Q_A^{-\bullet}$ charge recombination rate and TL properties [22,27,33] whereas the single Q130E mutation in *Synechocystis* 6803 and E130Q mutation in *Chlamydomonas reinhardtii* did [39–42].

The peak temperature of the glow curve has been shown here (Fig. 5) to be upshifted by ≈14 °C from ≈18 °C in PsbA3-PSII to ≈32 °C in PsbA3/E130Q. According to the empirical relationship between the shift in free energy and in the peak temperature discussed in [53,54], the expected shift in the E_m of the $Pheo_{D1}/Pheo_{D1}^{-\bullet}$ couple resulting from the E130 to Q130 single site directed mutation in

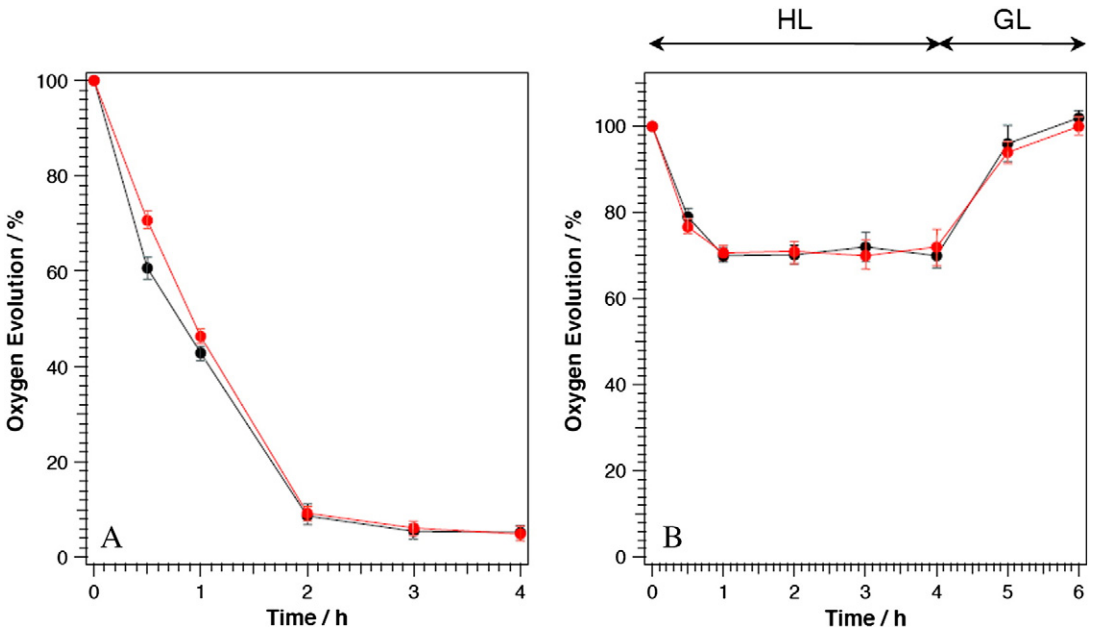

Fig. 7. Relative oxygen-evolving activity of WT*3 cells (black traces) and WT*3-E130Q cells (red traces) in the presence (Panel A) and in the absence (Panel B) of lincomycin. The activities are indicated in percentage relatively to the activities at 0 h. At t = 0, the activities were ≈300–350 μmol O_2 (mg Chl)$^{-1}$ h^{-1} in WT*3 cells and ≈350–400 μmol O_2 (mg Chl)$^{-1}$ h^{-1} in WT*3-E130Q cells. The activities under continuous saturating light intensity were measured by using the cells previously incubated under the high light conditions (HL = 800 μmol of photons m^{-2} s^{-1}) and then under growth light conditions (GL = 60 μmol of photons m^{-2} s^{-1}) at 45 °C. The results of 7 independent experiments with lincomycin and 3 independent experiments without lincomycin with different batches of cells have been averaged and the activity of each batch of cells has been measured 5 times.

PsbA3-PSII is ≈30 mV i.e. a downshift of similar extent as that observed in *C. reinhardtii* [42] upon the same single site directed mutagenesis and as that observed upon the Q130E single site directed mutagenesis in *Synechocystis* PCC 6803, although in the opposite direction [39,40,53].

The results obtained here, show that, reassuringly, the same cause has the same effect and that *T. elongatus* PSII does not escape this rule since the site-directed mutagenesis E130 to Q130 yielded similar effects as those observed previously mutation in *Synechocystis* 6803 and *C. reinhardtii* [39–42]. This brings supports to our earlier suggestion [22,33] that some or all of the 20 other additional amino-acid changes associated with the PsbA3 for PsbA1 substitution partly cancel the effect of the E130Q substitution on the E_m value of the $Pheo_{D1}/Pheo_{D1}^{-\bullet}$ couple since it increased by only 17 mV in PsbA3-PSII. Site-directed mutagenesis among other amino acid substitutions between PsbA1 and PsbA3 together with theoretical work, particularly quantum mechanical/molecular mechanical calculations, would be useful to decipher the influence of these 20 amino acids.

To reconcile the presence of PsbA3 under high light conditions with a higher E_m value for the $Pheo_{D1}/Pheo_{D1}^{-\bullet}$ couple, a condition that should facilitate the thermal repopulation of the $Pheo_{D1}^{-\bullet}Q_A$ state from the $Pheo_{D1}Q_A^{-\bullet}$ state and thus increase damaging ^{3}Chl formation [35], it was initially suggested [37] that a higher E_m ($Pheo/Pheo^{-\bullet}$) value in PsbA3-PSII would also favor charge recombination of the singlet state of the $P_{680}^{+\bullet}Pheo_{D1}^{-\bullet}$ radical pair at the expense of that of the triplet state thus disfavoring the production of harmful $^1O_2$ (see Fig. 1). This reasoning relied on the likely assumption that the charge recombination

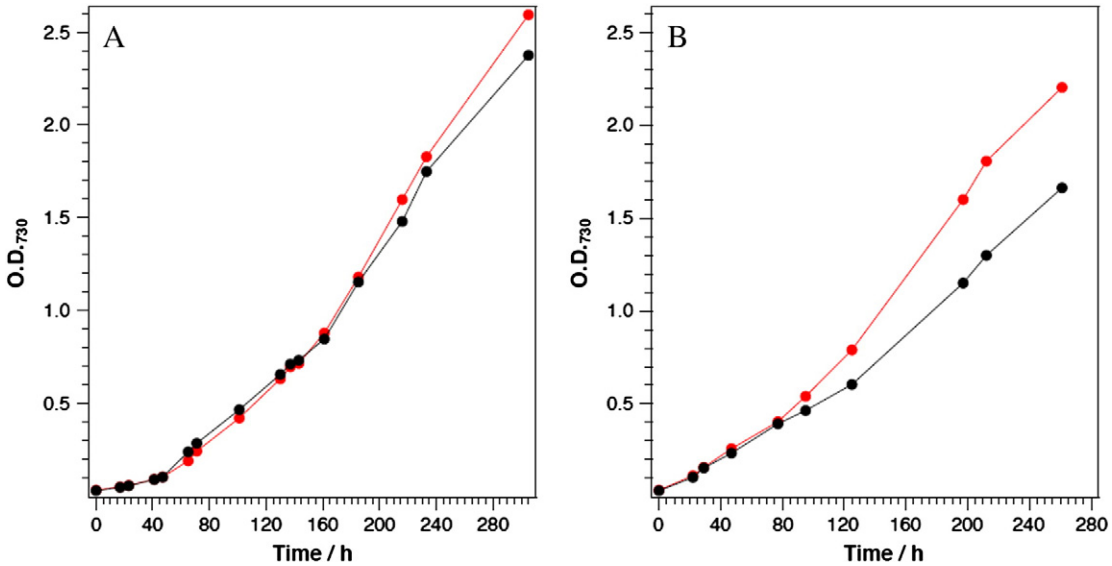

Fig. 8. Cell growth of WT*3 cell (black traces) and WT*3-E130Q cell (red traces) strains under the light condition of (A) 10 μmol of photons m^{-2} s^{-1} and (B) 80 μmol of photons m^{-2} s^{-1} at 45 °C.

between $Pheo^{-\bullet}$ and the donor-side occurs in the inverted region of the Marcus curve where the rate constants increase with decreasing driving force. For this hypothesis to be valid it required that the increased direct decay of $P_{680}^{+\bullet}Pheo_{D1}^{-\bullet}$ vs. the triplet route had to outweigh the increased repopulation of the $P_{680}^{+\bullet}Pheo_{D1}^{-\bullet}$ pair from the $P_{680}^{+\bullet}Pheo_{D1}Q_A^{-\bullet}$ state because of the smaller energy gap between them. This was discussed and it was suggested that the higher E_m of the Pheo/$Pheo^{-\bullet}$ couple might be better rationalized if the main recombination state occurring under high light were $P_{680}^{+\bullet}Pheo_{D1}^{-\bullet}Q_A^{-\bullet}$ rather than $P_{680}^{+\bullet}Pheo_{D1}Q_A^{-\bullet}$ [38]. In this case the energy gap between $P_{680}^{+\bullet}Pheo_{D1}Q_A^{-\bullet}$ and $P_{680}^{+\bullet}Pheo_{D1}^{-\bullet}$ would be less relevant and the faster decay of $P_{680}^{+\bullet}Pheo_{D1}^{-\bullet}$ vs. the triplet route would be a clear advantage. While this made sense for high light conditions, it did not resolve the problem of the smaller energy gap which would be predicted to give greater photodamage under lower light conditions. This was resolved when it was discovered that PsbA3-PSII unexpectedly had a higher E_m for the $Q_A/Q_A^{-\bullet}$ couple, upshifted compared to that in PsbA1-PSII by ≈41 mV [33].

Since this increase in the E_m for the $Q_A/Q_A^{-\bullet}$ couple is larger than that in the E_m of the Pheo/$Pheo^{-\bullet}$, couple the energy gap between $Pheo_{D1}Q_A^{-\bullet}$ and $Pheo_{D1}^{-\bullet}Q_A$ is expected to be larger in PsbA3-PSII than in PsbA1-PSII. This larger energy gap is expected to make the thermal repopulation of the $^3[P_{680}^{+\bullet}Pheo_{D1}^{-\bullet}]$ state from the $[P_{680}^{+\bullet}Q_A^{-\bullet}]$ state less probable. We have shown that, at least at cryogenic temperatures, the direct recombination involving $Q_A^{-\bullet}$ occurs in the Marcus inverted region [36]. Thus, following the same reasoning as that made above for $Pheo_{D1}^{-\bullet}$, we suggest that the direct charge recombination between $Q_A^{-\bullet}$ and the donor side to be faster in PsbA3-PSII than in PsbA1-PSII and this, again, should decrease the yield of production of $^1O_2$. All these different expectations can be numerically assessed by the appropriate modeling of electron transfer reactions in PSII. Such modeling has been done previously by Moser et al. [56] who relied on the knowledge provided the X-ray structure of the distances between the different redox cofactors in PSII and applied their empirical ruler that allows electron transfer rates to be calculated when the distance between the electron donor and acceptor and the driving force of the reaction are known [56,57]. We followed a similar approach to compare the time courses of the redox changes of the main cofactors in PsbA1-PSII, PsbA3-PSII and PsbA3/E130Q-PSII. The forward electron transfer rates were estimated using the empirical formula derived by Moser and Dutton [56,57]: $\mathrm{Log}(k_f) = 13 - 0.6(R - 3.6) - 3.1(\lambda - \Delta G)^2 / \lambda - \Delta G / 0.06$ where R is the edge-to-edge distance between the electron donor and acceptor (in Å), ΔG is the free energy change associated with the reaction (in eV) and λ is the reorganization energy (in eV). R was taken from the Photosystem II atomic structure PDB: 3ARC [1]. The various parameters used in the simulations have been adjusted so as to mimic as closely as possible the redox changes of the various cofactors involved in Photosystem II function, while keeping these parameters as close as possible to their experimental values when this one is known with sufficient accuracy. The set of differential equations that describe the above set of individual reactions was simulated numerically using the Copasi software (see Supplementary material for the value of these parameters). The three studied cases differed only in terms of the E_m values for Pheo/$Pheo^{-\bullet}$ and $Q_A/Q_A^{-\bullet}$. The time courses of the redox changes of the cofactors involved in the electron transfer reactions in PSII are shown in Fig. 9. These have been discussed in detail in [56] and here our main conclusion is that the computed time-course satisfyingly resembles that experimentally observed and that the changes in the energy level of $Pheo^{-\bullet}$ or $Q_A^{-\bullet}$ have only limited impact on the overall turnover of the enzyme. In particular they hardly affect the quantum efficiency as characterized by the yield of $S_2Q_A^{-\bullet}$ formation. This is consistent with the results in Fig. 4, which show that the period four oscillations are hardly changed by the E130Q mutation and with previous reports [58] in which the Q130E change barely affected the nanosecond quantum yield of radical pair formation.

Fig. 10 shows the simulated kinetics for $S_2Q_A^{-\bullet}$ charge recombination and on the associated formation of singlet oxygen. This was obtained by adding in the model two routes for the decay of the ^{3}Chl triplet state formed upon charge recombination of the $P_{680}^{+\bullet}Pheo_{D1}^{-\bullet}$ state: one associated with $^1O_2$ formation, with a rate constant of $3 \cdot 10^4\ s^{-1}$ [59], and the other one associated with the formation of the ground state with a rate constant of 600 s^{-1}, so that every single ^{3}P formed yields singlet oxygen with a probability of 98% [59]. These values were obtained from isolated D1/D2/Cytb_{559} reaction centers and these are significantly modified compared to intact PSII. They lack quinones, iron and Tyr function and more than 20 flanking and capping subunits. It is quite likely that the reactivity of the triplet bearing chlorophyll is somewhat different in the two cases. The present values for triplet yield are presented here with the proviso that the actual numbers may be different, probably over estimated. The computed time-course for $S_2Q_A^{-\bullet}$ charge recombination qualitatively match the trend observed experimentally: the PsbA1 (Q130) and PsbA3 (E130) only slightly differ and the PsbA3/E130Q shows a more pronounced slowdown of the radical pair decay. The more noticeable difference between PsbA1 and PsbA3 is the faster decay in PsbA3-PSII of the singlet radical pair $^1[P_{680}^{+\bullet}Pheo_{D1}^{-\bullet}]$ to the ground state which decreases the yield of $^3P_{680}$ formation. The more noticeable difference between PsbA3-PSII and PsbA3/E130Q-PSII is the rate for $[P_{680}^{+\bullet}Pheo_{D1}^{-\bullet}]$ (singlet + triplet) formation. Finally, the yield of singlet oxygen formation is ~60%, ~20% and ~7% in PsbA1-PSII, PsbA3-PSII, PsbA3/E130Q-PSII, respectively. This qualitatively correlates with the differential sensitivity to high light for PsbA1 vs. PsbA3, e.g. [44], and as we have shown here with the lack of detectable difference between PsbA3 and PsbA3/E130Q.

As a shift by approximately 30 mV can be easily achieved by a single amino acid substitution, we have simulated what would be the consequences of such a shift in the PsbA1 context (i.e. with the midpoint potential of $Q_A/Q_A^{-\bullet}$ being −120 mV and that of Pheo/$Pheo^{-\bullet}$ being downshifted by 30 mV, $E_m \approx -552$ mV). The simulation shows that the singlet oxygen yield is similarly decreased to that upon shifting from PsbA1 to PsbA3. Yet, the lifetime of the radical pair is strongly increased (see Supplementary material). In search of a rationalization for the evolutionary advantage for the presence of multiple mutations between the PsbA1 and PsbA3 genes rather than the single Q to E change at position 130, the reason could be that it is more "advantageous" to decrease the singlet oxygen yield without affecting too much the decay of $S_2Q_A^{-\bullet}$ state. Indeed, it seems likely that a longer-lived $S_2Q_A^{-\bullet}$ state would increase the probability that either S_2 and/or $Q_A^{-\bullet}$ get involved in unwanted reactions.

The sensitivity of PSII to high light intensity has been found to be different with PsbA1 (WT*1) or PsbA3 (WT*3) as the D1 protein [27,44,55]. When the cells were cultivated under high light conditions the following results were found [44][1]: (i) The O_2 evolution activity decreased faster in WT*1 cells than in WT*3 cells both in the absence and in the presence of lincomycin, a protein synthesis inhibitor; (ii) In WT*1 cells, the rate constant for the decrease of the O_2 evolution activity was comparable in the presence and in the absence of lincomycin; (iii) The D1 content monitored by western blot analysis decayed similarly in both WT*1 and WT*3 cells and much more slowly than O_2 evolution; and (iv) The faster decrease in O_2 evolution in WT*1 than in WT*3 cells correlated with a much faster inhibition of the S_2-state formation. All these results were in agreement with a photo-inhibition process resulting in the loss of the O_2 activity much faster than the D1 turnover in PsbA1-PSII and this seems likely to correspond to a greater production of reactive oxygen species under high light conditions in WT*1 than in WT*3. However, the finding that the recovery of the O_2 evolution under low light intensity is faster in WT*3 cells than in WT*1 cells [27,44], seems inconsistent with the observation that under the same

[1] It should be noted that in our previous work [44] the WT*1 strain had only the *psbA*$_1$ gene whereas in [27] the strain expressing PsbA1 contained both the *psbA*$_1$ and *psbA*$_2$ genes. We have indeed observed that the lag phase of the growth curve of the *psbA*$_3$-deleted mutant cells, containing both the *psbA*$_1$ and *psbA*$_2$ genes, was shorter than that of WT*1 cells (that contain only the *psbA*$_1$ gene) under the illumination of 60 μmol photons m^{-2} s^{-1}. This result suggests that the *psbA*$_2$ gene could be possibly transcribed during the lag phase in the *psbA*$_3$-deleted mutant [27].

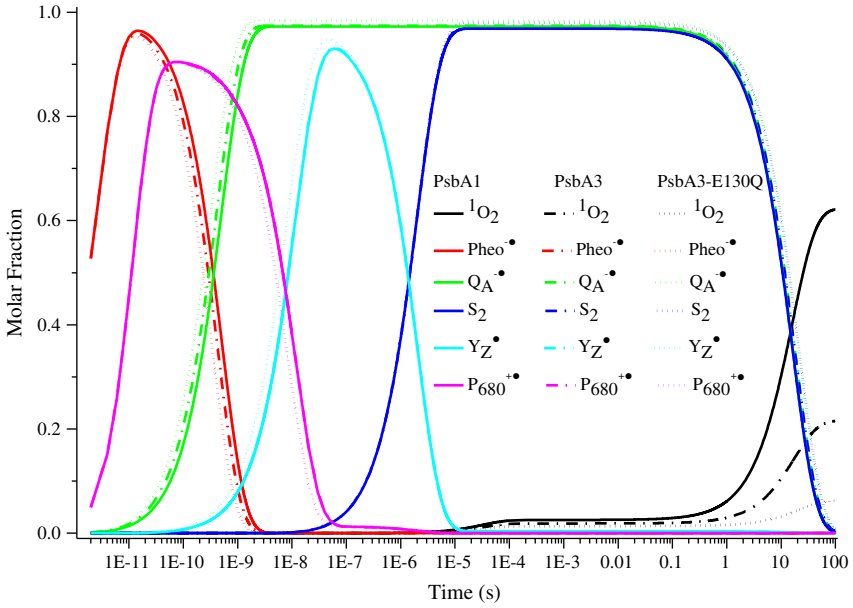

Fig. 9. Electron tunneling simulations of PSII electron transfer on a logarithmic scale after a flash illumination.

low light intensity the PSII in WT cells is constituted of PsbA1. So it appears that PsbA3 is not expressed when the 3 genes are present whereas it is expressed, even under low light, when the *psbA*$_1$ and *psbA*$_2$ genes are deleted. As a tentative explanation we proposed that (i) the expression of the *psbA*$_3$ gene in WT cells is down-regulated by the expression of the *psbA*$_1$ gene and (ii) strong light intensities inhibit the transcription of *psbA*$_1$ which in turn cancels the down-regulation of the *psbA*$_3$ transcription. The mechanism for such a regulation remains to be identified.

One of the important features in the response of WT*1 and WT*3 cells to environmental changes is that the *psbA*$_1$ and *psbA*$_3$ genes do not have the same promoter and this allows their transcription to be regulated independently. In contrast to this, in the present study the *psbA*$_3$ gene and the gene encoding PsbA3/E130Q have the same promoter. Thus the effects of the E130 to Q130 substitution on the sensitivity to high light conditions can be assigned to the structural changes this mutation induces without additional contributions from changes in the transcription level of the corresponding genes. Using a heterologous expression system for the two D1 isoforms of PsbA of *Synechococcus elongatus PCC 7942* in the green alga *C. reinhardtii*, showed functional advantages when D1:1-PSII and D1:2-PSII were expressed at low and high light regimes, respectively [60]. It has also been shown recently in *Synechocystis* 6803 that a D1-Q130E mutant appeared to produce less $^1O_2$ concomitantly with a decreased rate of the photodamage relative to the wild type [55].

From these results and those discussed above, we expected that in *T. elongatus* the WT*3/E130Q cells would exhibit greater resistance to high light conditions than the WT*3 cells. Although the growth rates of WT*3/E130Q cells were slightly faster than WT*3 cells even with a light intensity equal to 80 μmol of photons m^{-2} s^{-1}, the resistance under a high light intensity (800 μmol of photons m^{-2} s^{-1}) was hardly affected.

The present data and those obtained in *Synechocystis* 6803 can yet be reconciled. First, the light intensity used may differ in the various experiments reported in the literature. This will influence the steady state concentration of $Pheo_{D1}^{-\bullet}Q_A^-$ vs. $Pheo_{D1}Q_A^{-\bullet}$ and thus the sensitivity of the $^1O_2$ yield on the E130Q mutation. At higher light intensities $Pheo_{D1}^{-\bullet}Q_A^-$ is accumulated, the energy gap between $Pheo_{D1}Q_A^{-\bullet}$ and $Pheo_{D1}^{-\bullet}Q_A$ has little consequence on the $^1O_2$ yield, whereas the E_m of Pheo/Pheo$^{-\bullet}$ will influence the direct recombination rate in competition with the triplet route [38]. Under lower light intensities, both the energy gap between $Pheo_{D1}Q_A^{-\bullet}$ and $Pheo_{D1}^{-\bullet}Q_A$ and the E_m value of Pheo/Pheo$^{-\bullet}$ matter. If we consider that in our case, the accumulated state is $Pheo_{D1}Q_A^{-\bullet}$ (as in the simulations shown above), the benefit of a larger energy gap between $Pheo_{D1}Q_A^{-\bullet}$ and $Pheo_{D1}^{-\bullet}Q_A$ (41 mV) in PsbA3/E130Q-PSII compared to that in PsbA3-PSII (26 mV) is likely offset by the disadvantage of a much lower value by 30 mV for the E_m of Pheo/Pheo$^{-\bullet}$. The case where $Pheo_{D1}^{-\bullet}Q_A^-$ is photoaccumulated is unlikely because we would expect more photodamage something that is not observed. Finally, the fact that the downshift by 30 mV of the E_m of Pheo/Pheo$^{-\bullet}$ in PsbA3/E130Q-PSII did not decrease the rate of the photodamage of the cells when compared to WT*3 cells could suggest that in *T. elongatus* and in PsbA3-PSII the E_m of Pheo/Pheo$^{-\bullet}$ is not the only important parameter in the protection against photodamage. It is possible that the other 20 amino acid changes occurring within the PsbA1 to PsbA3 swap could play a totally different protective role.

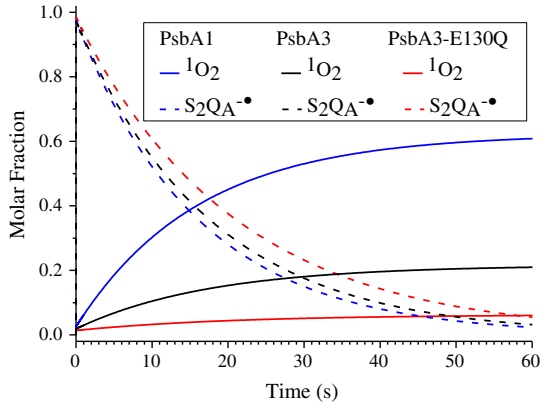

Fig. 10. Simulations for the $S_2Q_A^-$ charge recombination kinetics (dashed lines) and $^1O_2$ production (continuous lines) in PsbA1-PSII (blue traces), PsbA3-PSII (black traces) and PsbA3/E130Q-PSII (red traces). See the text for more details and Supplementary material for the electron tunneling simulations of PSII electron transfer for all species after a flash illumination.

Acknowledgements

Jean-Marc Ducruet is acknowledged for his help in TL measurements. Yui Ozaki (Ehime University) is acknowledged for technical support. A.B. was supported in part by a CEA/DSV-Bioenergy grant. M.S. was supported by the JST-PRESTO program (4018). AWR is supported by BBSRC Research Grant BB/K002627/1. FR acknowledges financial support from the CNRS and the "Initiative d'Excellence" program from the French State (Grant "DYNAMO", ANR-11-LABX-0011-01).

Appendix A. Supplementary data

Supplementary data to this article can be found online at http://dx.doi.org/10.1016/j.bbabio.2013.09.009.

References

[1] Y. Umena, K. Kawakami, J.-R. Shen, N. Kamiya, Crystal structure of oxygen-evolving Photosystem II at a resolution of 1.9 Å, Nature 473 (2011) 55–60.
[2] B.A. Diner, F. Rappaport, Structure, dynamics, and energetic of the primary photochemistry of photosystem II of oxygenic photosynthesis, Annu. Rev. Plant Biol. 53 (2002) 551–580.
[3] G. Renger, Light-induced oxidative water splitting in photosynthesis: energetics, kinetics, and mechanism, J. Photochem. Photobiol. B 104 (2011) 35–43.
[4] M.L. Groot, N.P. Pawlowicz, L.J. van Wilderen, J. Breton, I.H. van Stokkum, R. van Grondelle, Initial electron donor and acceptor in isolated Photosystem II reaction centers identified with femtosecond mid-IR spectroscopy, Proc. Natl. Acad. Sci. U. S. A. 102 (2005) 13087–13092.
[5] A.R. Holzwarth, M.G. Muller, M. Reus, M. Nowaczyk, J. Sander, M. Rogner, Kinetics and mechanism of electron transfer in intact Photosystem II and in the isolated reaction center: pheophytin is the primary electron acceptor, Proc. Natl. Acad. Sci. U. S. A. 103 (2006) 6895–6900.
[6] B. Kok, B. Forbush, M. McGloin, Cooperation of charges in photosynthetic O_2 evolution—I. A linear four step mechanism, Photochem. Photobiol. 11 (1970) 457–475.
[7] P. Joliot, B. Kok, Oxygen evolution in photosynthesis, in: Govindjee (Ed.), Bioenergetics of Photosynthesis, Academic Press, New York, 1975, pp. 387–412.
[8] H. Dau, I. Zaharieva, M. Haumann, Recent developments in research on water oxidation by Photosystem II, Curr. Opin. Chem. Biol. 16 (2012) 3–10.
[9] N. Cox, J. Messinger, Reflections on substrate water and dioxygen formation, Biochim. Biophys. Acta 1827 (2013) 1020–1030.
[10] N. Cox, D.A. Pantazis, F. Neese, W. Lubitz, Biological water oxidation, Acc. Chem. Res. 46 (2013) 1588–1596.
[11] P. Glatzel, H. Schroeder, Y. Pushkar, T. Boron, S. Mukherjee, G. Christou, V.L. Pecoraro, J. Messinger, V.K. Yachandra, U. Bergmann, J. Yano, Electronic structural changes of Mn in the oxygen-evolving complex of Photosystem II during the catalytic cycle, Inorg. Chem. 52 (2013) 5642–5644.
[12] H.J. van Gorkom, Electron transfer in photosystem II, Photosynth. Res. 6 (1985) 97–111.
[13] M. Grabolle, H. Dau, Energetics of primary and secondary electron transfer in Photosystem II membrane particles of spinach revisited on basis of recombination-fluorescence measurements, Biochim. Biophys. Acta 1708 (2005) 209–218.
[14] G. Renger, Mechanism of light induced water splitting in Photosystem II of oxygen evolving photosynthetic organisms, Biochim. Biophys. Acta 1817 (2012) 1164–1176.
[15] A.K. Clarke, A. Soitamo, P. Gustafsson, G. Oquist, Rapid interchange between two distinct forms of cyanobacterial photosystem II reaction-center protein D1 in response to photoinhibition, Proc. Natl. Acad. Sci. U. S. A. 90 (1993) 9973–9977.
[16] S.S. Golden, Light-responsive gene expression in cyanobacteria, J. Bacteriol. 177 (1995) 1651–1654.
[17] J. Komenda, H. Hassan, B.A. Diner, R.J. Debus, J. Barber, P.J. Nixon, Degradation of the Photosystem II D1 and D2 proteins in different strains of the cyanobacterium *Synechocystis* PCC 6803 varying with respect to the type and level of *psbA* transcript, Plant Mol. Biol. 42 (2000) 635–645.
[18] C.I. Sicora, S.E. Appleton, C.M. Brown, J. Chung, J. Chandler, A.M. Cockshutt, I. Vass, D.A. Campbell, Cyanobacterial *psbA* families in *Anabaena* and *Synechocystis* encode trace, constitutive, and UVB-induced D1 isoforms, Biochim. Biophys. Acta 1757 (2006) 47–56.
[19] P.B. Kós, Z. Deák, O. Cheregi, I. Vass, Differential regulation of *psbA* and *psbD* gene expression, and the role of the different D1 protein copies in the cyanobacterium *Thermosynechococcus elongatus* BP-1, Biochim. Biophys. Acta 1777 (2008) 74–83.
[20] P. Mulo, C. Sicora, E.-M. Aro, Cyanobacterial *psbA* gene family: optimization of oxygenic photosynthesis, Cell. Mol. Life Sci. 66 (2009) 3697–3710.
[21] C.I. Sicora, F.M. Ho, T. Salminen, S. Styring, E.-M. Aro, Transcription of a "silent" cyanobacterial *psbA* gene is induced by microaerobic conditions, Biochim. Biophys. Acta 1787 (2009) 105–112.
[22] M. Sugiura, Y. Kato, R. Takahashi, H. Suzuki, T. Watanabe, T. Noguchi, F. Rappaport, A. Boussac, Energetics in Photosystem II from *Thermosynechococcus elongatus* with a D1 protein encoded by either the $psbA_1$ or $psbA_3$ gene, Biochim. Biophys. Acta 1797 (2010) 1491–1499.
[23] E. Kiss, P.B. Kos, M. Chen, I. Vass, A unique regulation of the expression of the *psbA*, *psbD*, and *psbE* genes, encoding the D1, D2 and cytochrome b_{559} subunits of the Photosystem II complex in the chlorophyll d containing cyanobacterium *Acaryochloris marina*, Biochim. Biophys. Acta 1817 (2012) 1083–1094.
[24] D.J. Vinyard, J. Gimpel, G.M. Ananyev, M.A. Cornejo, S.S. Golden, S.P. Mayfield, G.C. Dismukes, Natural variants of Photosystem II subunit D1 tune photochemical fitness to solar intensity, J. Biol. Chem. 288 (2013) 5424–5462.
[25] Y. Nakamura, T. Kaneko, S. Sato, M. Ikeuchi, H. Katoh, S. Sasamoto, A. Watanabe, M. Iriguchi, K. Kawashima, T. Kimura, Y. Kishida, C. Kiyokawa, M. Kohara, M. Matsumoto, A. Matsuno, N. Nakazaki, S. Shimpo, M. Sugimoto, C. Takeuchi, M. Yamada, S. Tabata, Complete genome structure of the thermophilic cyanobacterium *Thermosynechococcus elongatus* BP-1, DNA Res. 9 (2002) 123–130.
[26] B. Loll, M. Broser, P.B. Kós, J. Kern, J. Biesiadka, I. Vass, W. Saenger, A. Zouni, Modeling of variant copies of subunit D1 in the structure of Photosystem II from *Thermosynechococcus elongatus*, Biol. Chem. 389 (2008) 609–617.
[27] J. Sander, M. Nowaczyk, J. Buchta, H. Dau, I. Vass, Z. Deak, M. Dorogi, M. Iwai, M. Rogner, Functional characterization and quantification of the alternative PsbA copies in *Thermosynechococcus elongatus* and their role in photoprotection, J. Biol. Chem. 285 (2010) 29851–29856.
[28] T.C. Summerfield, J. Toepel, L.A. Sherman, Low-oxygen induction of normally cryptic *psbA* genes in cyanobacteria, Biochemistry 47 (2008) 12939–12941.
[29] X. Zhang, L.A. Sherman, Alternate copies of D1 are used by cyanobacteria under different environmental conditions, Photosynth. Res. 114 (2012) 133–135.
[30] J.W. Murray, Sequence variation at the oxygen-evolving centre of photosystem II: a new class of 'rogue' cyanobacterial D1 proteins, Photosynth. Res. 110 (2012) 177–184.
[31] P. Mulo, I. Sakurai, E.-M. Aro, Strategies for psbA gene expression in cyanobacteria, green algae and higher plants: from transcription to PSII repair, Biochim. Biophys. Acta 1817 (2012) 247–257.
[32] Y. Kato, M. Sugiura, A. Oda, T. Watanabe, Spectroelectrochemical determination of the redox potential of pheophytin a, the primary electron acceptor in Photosystem II, Proc. Natl. Acad. Sci. U. S. A. 106 (2009) 17365–17370.
[33] Y. Kato, T. Shibamoto, S. Yamamoto, T. Watanabe, N. Ishida, M. Sugiura, F. Rappaport, A. Boussac, Influence of the PsbA1/PsbA3 and Ca^{2+}/Sr^{2+} or Cl^-/Br^- exchanges on the redox potential of the primary quinone Q_A in Photosystem II as revealed by spectroelectrochemistry, Biochim. Biophys. Acta 1817 (2012) 1998–2004.
[34] Y. Kato, T. Shibamoto, S. Yamamoto, T. Watanabe, N. Ishida, M. Sugiura, F. Rappaport, A. Boussac, Influence of the PsbA1/PsbA3, Ca^{2+}/Sr^{2+} and Cl^-/Br^- exchanges on the redox potential of the primary quinone Q_A in Photosystem II from *Thermosynechococcus elongatus* as revealed by spectroelectrochemistry, Biochim. Biophys. Acta 1817 (2012) 1998–2004.
[35] G.N. Johnson, A.W. Rutherford, A. Krieger, A change in the midpoint potential of the quinone Q_A in Photosystem II associated with photoactivation of oxygen evolution, Biochim. Biophys. Acta 1229 (1995) 202–207.
[36] A. Boussac, F. Rappaport, K. Brettel, M. Sugiura, Marcus inverted region behavior of very long distance electron tunneling in Photosystem II, J. Phys. Chem. B 117 (2013) 3308–3314.
[37] I. Vass, K. Cser, Janus-faced charge recombinations in Photosystem II photoinhibition, Trends Plant Sci. 14 (2009) 200–205.
[38] A.W. Rutherford, A. Osyczka, F. Rappaport, Back-reactions, short-circuits, leaks and other energy wasteful reactions in biological electron transfer; redox tuning for life in O_2, FEBS Lett. 586 (2012) 603–616.
[39] S.A.P. Merry, P.J. Nixon, L.M.C. Barter, M. Schilstra, G. Porter, J. Barber, J.R. Durrant, D.R. Klug, Modulation of quantum yield of primary radical pair formation in Photosystem II by site-directed mutagenesis affecting radical cations and anions, Biochemistry 37 (1998) 17439–17447.
[40] F. Rappaport, M. Guergova-Kuras, P.J. Nixon, B.A. Diner, J. Lavergne, Kinetics and pathways of charge recombination in Photosystem II, Biochemistry 41 (2002) 8518–8527.
[41] A. Cuni, L. Xiong, R. Sayre, F. Rappaport, J. Lavergne, Modification of the pheophytin midpoint potential in Photosystem II: modulation of the quantum yield of charge separation and of charge recombination pathways, Phys. Chem. Chem. Phys. 6 (2004) 4825–4831.
[42] F. Rappaport, A. Cuni, L. Xiong, R. Sayre, J. Lavergne, Charge recombination and thermoluminescence in Photosystem II, Biophys. J. 88 (2005) 1948–1958.
[43] M. Sugiura, A. Boussac, T. Noguchi, F. Rappaport, Influence of Histidine-198 of the D1 subunit on the properties of the primary electron donor, P680, of photosystem II in *Thermosynechococcus elongatus*, Biochim. Biophys. Acta 1777 (2008) 331–342.
[44] S. Ogami, A. Boussac, M. Sugiura, Deactivation processes in PsbA1-Photosystem II and PsbA3-Photosystem II under photoinhibitory conditions in the cyanobacterium *Thermosynechococcus elongatus*, Biochim. Biophys. Acta 1817 (2012) 1322–1330.
[45] J.-M. Ducruet, Chlorophyll thermoluminescence of leaf discs: simple instruments and progress in signal interpretation open the way to new ecophysiological indicators, J. Exp. Bot. 54 (2003) 2419–2430.
[46] J.-M. Ducruet, I. Vass, Thermoluminescence: experimental, Photosynth. Res. 201 (2009) 195–204.
[47] D. Beal, F. Rappaport, P. Joliot, A new high-sensitivity 10-ns time-resolution spectrophotometric technique adapted to in vivo analysis of the photosynthetic apparatus, Rev. Sci. Instrum. 70 (1999) 202–207.
[48] J.L. Hughes, N. Cox, A.W. Rutherford, E. Krausz, T.-L. Lai, A. Boussac, M. Sugiura, D1 protein variants in Photosystem II from *Thermosynechococcus elongatus* studied by low temperature optical spectroscopy, Biochim. Biophys. Acta 1797 (2010) 11–19.
[49] Y. Shibuya, R. Takahashi, T. Okubo, H. Suzuki, M. Sugiura, T. Noguchi, Hydrogen bond interaction of the pheophytin electron acceptor and its radical anion in Photosystem II as revealed by Fourier Transform Infrared Difference Spectroscopy, Biochemistry 49 (2010) 493–501.
[50] N. Ishida, M. Sugiura, F. Rappaport, T.-L. Lai, A.W. Rutherford, A. Boussac, Biosynthetic exchange of bromide for chloride and strontium for calcium in the Photosystem II oxygen-evolving enzyme, J. Biol. Chem. 283 (2008) 13330–13340.

[51] J. Lavergne, Absorption changes of Photosystem-II donors and acceptors in algal cells, FEBS Lett. 173 (1984) 9–14.
[52] J. Lavergne, Improved UV–visible spectra of the S-transitions in the photosynthetic oxygen-evolving system, Biochim. Biophys. Acta 1060 (1991) 175–188.
[53] K. Cser, I. Vass, Radiative and non-radiative charge recombination pathways in Photosystem II studied by thermoluminescence and chlorophyll fluorescence in the cyanobacterium *Synechocystis* 6803, Biochim. Biophys. Acta 1767 (2007) 233–243.
[54] F. Rappaport, J. Lavergne, Thermoluminescence: theory, Photosynth. Res. 101 (2009) 205–216.
[55] A.U. Rehman, K. Cser, L. Sass, I. Vass, Characterization of singlet oxygen production and its involvement in photodamage of Photosystem II in the cyanobacterium *Synechocystis* PCC 6803 by histidine-mediated chemical trapping, Biochim. Biophys. Acta 1827 (2013) 689–698.
[56] C.C. Moser, C.C. Page, P.L. Dutton, Tunneling in PSII, Photochem. Photobiol. Sci. 12 (2005) 933–939.
[57] C.C. Moser, P.L. Dutton, Protein Electron Transfer in Outline of Theory of Protein Electron Transfer, in: D.S. Bendal (Ed.), BIOS Scientific Publishers Ltd., Oxford, 1996, pp. 1–21.
[58] L.B. Giorgi, P.J. Nixon, S.A.P. Merry, D.M. Joseph, J.R. Durrant, J.D. Rivas, J. Barber, G. Porter, D.R. Klug, Comparison of primary charge separation in the Photosystem II reaction center complex isolated from wild-type and D1-130 mutants of the cyanobacterium *Synechocystis* PCC 6803, J. Biol. Chem. 271 (1996) 2093–2101.
[59] J.R. Durrant, L.B. Giorgi, J. Barber, D.R. Klug, G. Porter, Characterisation of triplet states in isolated Photosystem II reaction centres: oxygen quenching as a mechanism for photodamage, Biochim. Biophys. Acta 1017 (1990) 167–175.
[60] D.J. Vinyard, J. Gimpel, G.M. Ananyev, M.A. Cornejo, S.S. Golden, S.P. Mayfield, G.C. Dismukes, Natural variants of Photosystem II subunit D1 tune photochemical fitness to solar intensity, J. Biol. Chem. 288 (2013) 5451–5462.